Vesicles

DOI: 10.1002/anie.201103164

Reversible and Large-Scale Cytomimetic Vesicle Aggregation: Light-Responsive Host–Guest Interactions**

Haibao Jin, Yongli Zheng, Yong Liu, Haixing Cheng, Yongfeng Zhou, and Deyue Yan*

Cell aggregation or cellular agglomeration through specific intracellular molecular recognition plays a critical role in a wide array of biological processes which include hemostasis, immune response, inflammation embryogenesis, and the development of neuronal tissue.[1] However, despite the great significance, it is very difficult to directly investigate the cell aggregation because of the complexity of the biomembranes and proteins involved. Recently, synthetic vesicles have been demonstrated to be excellent model membranes for mimicking the dynamic and structural features of cellular processes, and disclosing the mechanisms therein, such as adhesion, fusion, fission, endocytosis, budding, and birthing; this has become a blossoming field coined cytomimetic chemistry as reviewed by Menger et al.[2] As a part of cytomimetic chemistry, vesicle–vesicle aggregation for mimicking cell aggregation processes has also received much attention. The groups of Lehn,[3] Menger,[4] Paleos,[5] Ravoo,[6] Webb,[7] Kim,[8] as well as others have done excellent work on vesicle aggregation. However, up to now, most of the work is limited to the aggregation of liposomes or surfactant vesicles with submicroscopic sizes, and the scale of the reported vesicle aggregates is smaller than 100 micrometers. However, in nature, the cells are generally micrometer sized and may form huge aggregates such as tissues, on the macroscopic scale in the body. Thus, mimicking large-scale cell aggregation using giant vesicles having a cell-like size (1–200 μm) as model membranes has been greatly anticipated, but hardly performed.

Polymer vesicles (polymersomes) that self-assembled from linear block copolymers have received much attention in recent years because of their special properties and applications when compared to those of liposomes.[9] However, only limited work on the aggregation of polymersomes has been reported by the groups of Discher,[10] Hammer,[11] Balazs,[12] and Ryan et al.[13] Very recently, we developed a new type of polymer vesicle, coined "branched polymersomes" (BPs), that arises from the self-assembly of amphiphilic hyperbranched multiarm copolymers.[14] BPs possess the combined properties, such as good membrane fluidity and strong stability, of liposomes and polymersomes, and have demonstrated the potential to be excellent model membranes for mimicking cellular fusion and fission process.[15] In addition since hyperbranched polymers have a large population of functional groups, such as dendrimers, BPs have the inherent advantage of possessing multivalent intervesicular interactions, and they may be very promising model systems for mimicking cell aggregation processes.[16] Nevertheless, to our knowledge, no work has been reported on cytomimetic aggregation based on hyperbranched polymer vesicles to date.

Herein, we report for the first time a large-scale vesicle aggregation process by using giant BPs as the building blocks, and we were able to directly observe the process by optical microscopy because of the large vesicle size. As shown in Scheme 1, two populations of BPs, one functionlized with β-cyclodextrin (CD-BPs) and the other with azobenzene (Azo-BPs), were prepared through a coassembly method. They then aggregated through multivalent intervesicular host–guest interactions between the CD and Azo groups.[17,6d] The vesicle aggregation process was not only highly efficient for obtaining large-scale macroscopic aggregates, but also totally reversible under alternating irradiation with UV and visible light (Vis). In addition, vesicle fusion events occurred frequently throughout the process and were observed in real time. Also, the aggregate dimension could be controlled through adjusting the vesicle concentration and composition.

We have previously reported the aqueous self-assembly of BPs from an amphiphilic hyperbranched multiarm copolymer of HBPO-star-PEO, where HBPO represents the hydrophobic hyperbranched poly(3-ethyl-3-oxetanemethanol) core

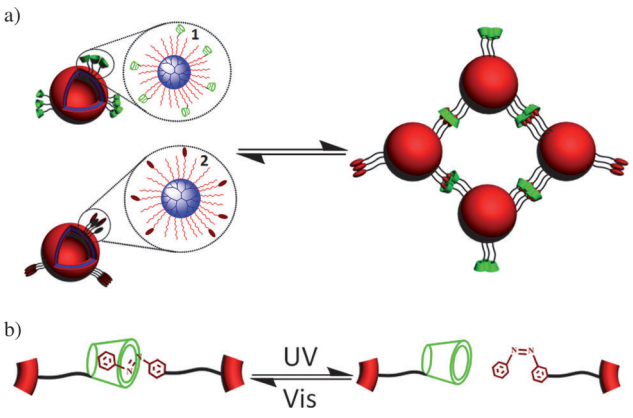

Scheme 1. a) Reversible aggregation of BPs. b) Light-responsive host–guest recognition between CD and azobenzene that triggers the aggregation.

[*] Dr. H. Jin, Y. Zheng, Y. Liu, H. Cheng, Prof. Y. Zhou, D. Yan
School of Chemistry and Chemical Engineering, State Key Laboratory of Metal Matrix Composites, Shanghai Jiao Tong University
800 Dongchuan Road, Shanghai 200240 (China)
E-mail: yfzhou@sjtu.edu.cn

[**] We thank the National Basic Research Program (2007CB808000, 2009CB930400), the National Natural Science Foundation of China (21074069, 20874060, and 50873058), the Foundation for the Author of National Excellent Doctoral Dissertation of China, and the Fok Ying Tung Education Foundation (No. 114029).

Supporting information for this article is available on the WWW under http://dx.doi.org/10.1002/anie.201103164.

and PEO represents the hydrophilic poly(ethylene oxide) arms. The vesicle size can be easily controlled, ranging from 100 nm to 100 μm by adjustment of the molar fraction (f_{EO}) of PEO.[14] To mimic the prokaryotic cells that are generally 1–10 μm in size, we selected the BP samples that were on average 5–10 μm in size according to the optical microscopy by the self-assembly of HBPO-star-PEO with $f_{EO} = 67\,\%$. The vesicle structure was carefully characterized by fluorescent microscopy, transmission electron microscopy (TEM), and small-angle X-ray scattering (SAXS) measurements (see Figures S10, S11, and S12, respectively, in the Supporting Information) which indicate that the BPs are unilamellar vesicles with a bilayer structure. The hollow lumens of the vesicles were additionally confirmed by dye encapsulation experiments (see Figures S13 and S14).

The functional species HBPO-star-PEO-CD (**1**) and HBPO-star-PEO-Azo (**2**) were synthesized through the end-group modification of HBPO-star-PEO (see Figures S1 and S2 in the Supporting Information). For the coassembly process, the HBPO-star-PEOs were homogeneously admixed with either **1** or **2** in the cosolvent chloroform, and then the dried mixtures were put into water to induce self-assembly; the final concentration was 5 mg mL^{-1}. As a result of the very similar structures, both **1** and **2** were expected to be spontaneously doped into the membranes of BPs to form mixed CD-BPs (1.25 mM of CD groups) and Azo-BPs (1.05 mM of Azo groups), respectively, through a coassembly process. However, no obvious changes in the vesicle size and morphology were observed after the coassembly (Figures 1 a and b) upon comparison with the single-component BPs. To discern these two mixed vesicles, the HBPO-star-PEOs in the CD-BPs were labeled with red fluorescent rhodamine B (HBPO-star-PEO-R_b; inset in Figure 1 a) and those in the Azo-BPs were labeled with green fluorescent dansyl chloride (HBPO-star-PEO-DNS; inset in Figure 1 b). Details of the sample syntheses, characterizations, and self-assembly are shown in the Supporting Information.

The mixed vesicle structure was confirmed by using fluorescence probe methods involving pyrene.[18] In the fluorescent spectra of pyrene-containing vesicles obtained through the self-assembly of pyrene-labeled HBPO-star-PEO (HBPO-star-PEO-Py; see Figure S5 in the Supporting Information), a strong excimer emission peak (I_E at $\lambda = 480$ nm) resulting from the tight contact of the pyrene chromophores was observed. With the introduction of **1** (or **2**) into the vesicles, the relative ratio of the excimer versus monomer (I_M at $\lambda = 398$ nm) fluorescence intensity (I_E/I_M) decreased with increasing amounts of **1** (or **2**; see Figures S14 and S15), which indicated that either **1** or **2** were inserted into the vesicle membranes, thus diluting the chromophores and forming the binary vesicles of either CD-BPs or Azo-BPs.

Vesicle aggregation was performed by mixing CD-BPs with Azo-BPs at a molar ratio of 1:0.84 with respect to the CD and Azo units. At first, the vesicle solution was yellow and homogeneously turbid (left bottle, Figure 1 c). After 24 hours, the solution became clear and a yellow coacervate formed (right bottle, Figure 1 c). The coacervate phase consisted of a macroscopic three-dimensional (3D) network of densely packed vesicles as disclosed by optical and fluorescent

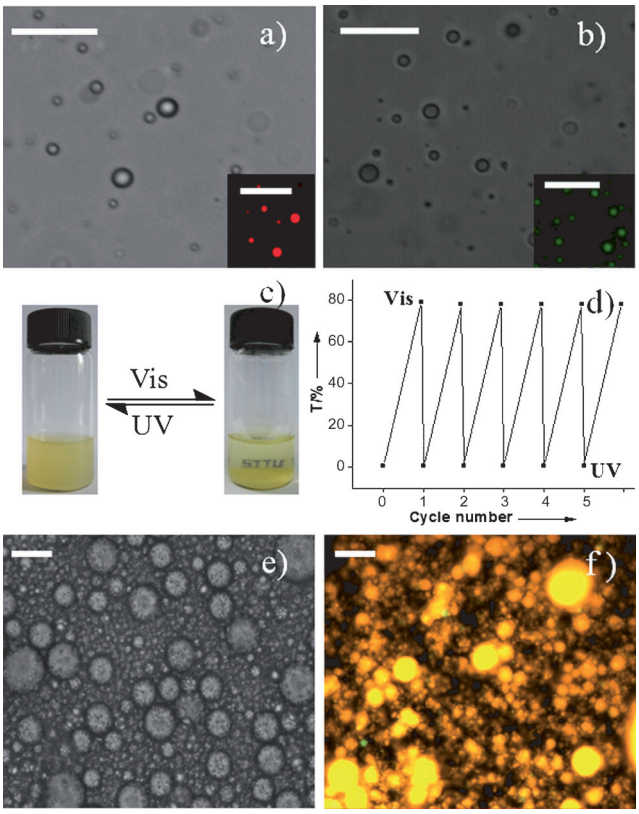

Figure 1. Optical micrographs and solution properties of the mixed vesicles. a) CD-BPs; b) Azo-BPs; c) The vesicle solution upon treatment with Vis and UV irradiation; d) Reversible changes of transmittance for the Vis and UV cycles; e) Optical micrograph of the large-scale vesicle aggregates from CD-BPs and Azo-BPs; f) Fluorescent overlay micrograph showing the colocalization of CD-BPs (red) and Azo-BPs (green) in the large-scale vesicle aggregates. Scale bars: 25 μm.

microscopy (Figures 1 e and 1 f, respectively). These observations indicated a highly efficient and large-scale aggregation among CD-BPs and Azo-BPs. We assumed that the vesicles were aggregated through the formation of multiple intervesicular host–guest interactions between the CD and Azo groups as shown in Scheme 1 a. As we know, only the *trans*-Azo can form host-guest inclusion with CD, whereas the *cis*-Azo cannot.[17a] Thus, if our hypothesis was right, the vesicles would undergo a reversible light-responsive aggregation and disaggregation process as shown in Scheme 1 b. Our experiments supported this hypothesis. Under alternating UV ($\lambda =$ 356 nm, for 1.5 h) and Vis (sun light, for 24 h) irradiation cycles, the coacervate disassociated into individual vesicles (see Figure S17 in the Supporting Information) and then re-aggregated into the coacervate (Figure 1 C); this was accompanied by a reversible change of the solution light transmittance (Figure 1 d). The hypothesis was additionally confirmed by adding a competitive host for α-CD into the system under Vis irradiation; no vesicle aggregation was observed, and the vesicle coacervate was changed into individual vesicles (see Figure S18).

Vesicle fusion occurred in the aggregation process. We captured a real-time membrane fusion event of two separated

vesicles as shown in Figure 2a. The whole fusion process lasted about 20 seconds and included four successive steps: membrane contact, formation of center wall, symmetric expanding of the fusion pore, and complete fusion.[15a] The content mixing assay based on the formation of a fluorescent Tb^{3+}/dipicolinic acid (DPA) complex was used to monitor the fusion process.[19] In this assay vesicle populations of CD-BPs and Azo-BPs were loaded with Tb^{3+} and DPA, respectively. A strong fluorescence attributed to the formation of a Tb-$(DPA)_3^{3-}$ complex through the mixing of the aqueous vesicle contents was observed during the aggregation of these Tb-CD-BPs and DPA-Azo-BPs, thereby confirming the fusion events (Figure 2b). A decrease in fluorescence owing to the quenching of the $Tb(DPA)_3^{3-}$ complex by a stronger ligand, EDTA, was observed, thus indicating the content leakage in the fusion process. As the control experiments, no aqueous content mixing was observed in the systems having Tb-CD-BPs and DPA-CD-BPs, or Tb-Azo-BPs and DPA-Azo-BPs, or Tb-CD-BPs and DPA-Azo-BPs in the presence of α-CD. Also, as further evidence for vesicle fusion, we showed that there was mixing of the vesicle polymer components during the aggregation of the pyrene-labeled CD-BPs and Azo-BPs through a typical pyrene excimer assay (see Figure S19 in the Supporting Information).[20] Such a result from component mixing was directly visualized by the fluorescence overlay micrograph of the orange vesicle aggregates (Figure 1f), because of the co-localization of red fluorescent CD-BPs and green fluorescent Azo-BPs. Thus, it can be concluded that the vesicle fusion is driven by the specific intervesicular recognition between the CD and Azo groups.

In addition, we also tracked the vesicle aggregation process by optical microscopy (see Figure S20 in the Supporting Information). Firstly, we found that the CD-BPs and Azo-BPs undergo sequential formation of dimers, multimers, linear chains, and then branched chains before achieving the final structure of a large vesicle network. Secondly, we found that vesicle fusion occurred frequently during the formation of the vesicle dimers or multimers. In other words, vesicle aggregation and fusion proceeded synchronously in our system. However, the vesicle fusion events could not proceed infinitely, and would therefore stop at some critical vesicle size, which made the final vesicle aggregates stable. In fact, the vesicle aggregates are stable under visible light for at least a half year (see Figure S21). We propose that at some stage all the CD and Azo units within the vesicles form intravesicular complexes, and thus the intervesicular molecular recognition is inhibited, and leads to the cesation of vesicle fusion cycles.

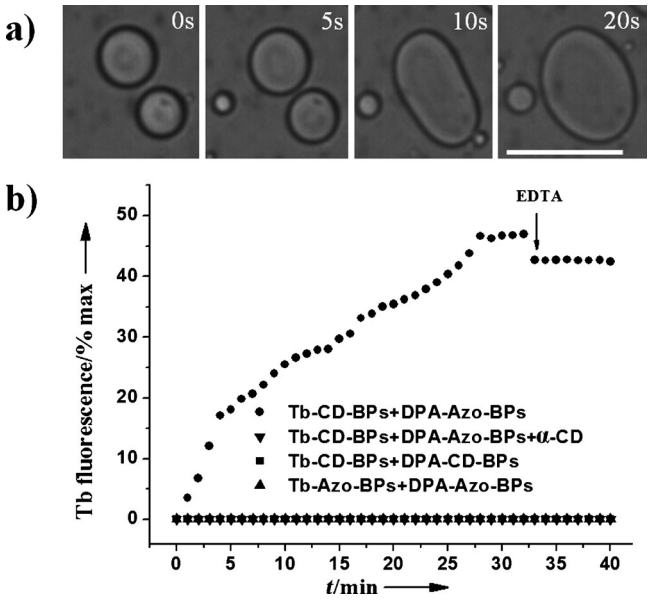

Figure 2. a) Real-time fusion sequences of two giant vesicles. b) The content mixing assay experiments. Scale: 25 μm.

We also studied the vesicle aggregation process at a molecular level. The ^{1}H NOESY spectrum of CD-BPs and Azo-BPs in D_2O at 25 °C (see Figure S22 in the Supporting Information) indicated that the Azo units bound within the hydrophobic cavity of the β CD rings to form host-guest inclusion complexes. The UV/Vis spectra of the mixed CD-BP/Azo-BP solution under Vis irradiation were measured at different time points at 25 °C. Only one absorption band at around $\lambda = 328$ nm was observed and assigned to the $\pi \rightarrow \pi^*$ transition of the *trans*-Azo groups, and it decreased as the irradiation time increased (Figure 3a). Thus, together with the ^{1}H NOESY results, it can be concluded that the driving force for the vesicle aggregation comes from the host-guest recognition between *trans*-Azo and CD units. In addition, Figure 3a also provides evidence for the formation of the vesicle aggregate. Since there was a solution-to-coacervate phase transition during the vesicle aggregation, it led to a decrease of the *trans*-Azo concentration in solution. Thus, as reflected in the UV/Vis spectra, the peak corresponding to the *trans*-Azo absorbance decreased accordingly.

Similarly, we tracked the vesicle disaggregation process by continuously measuring the UV/Vis spectra of the vesicle coacervate phase under UV irradiation at $\lambda = 356$ nm at different time points. In addition to the peak corresponding to the *trans*-Azo compound at $\lambda = 328$ nm, there is another absorption peak at around $\lambda = 430$ nm that is assigned to $n \rightarrow \pi^*$ transition of the *cis*-Azo groups (Figure 3b). To get quantitative information, the percentage rate of increase (R) of the absorbance for each peak was calculated by comparing the absorbance at a certain irradiation time (A_t) relative to that at time zero (A_0) using the equation $R = (A_t - A_0)/A_0$. Evidently, there is a pronounced increase in the intensity of the peak for the *cis*-Azo compound as the irradiation time increases, and there is only a small change observed for that of *trans*-Azo compound (inset of Figure 3b). The result indicates the isomerization of the azobenzene units from the *trans* form to the *cis* form after UV irradiation. As the *cis*-Azo units cannot be recognized by β-CD, they will escape from the cavity of the β-CD units and thus destroy the intervesicular host–guest interactions (Scheme 1b). Therefore, the vesicle disaggregation occurred and led to a coacervate-to-solution phase transition. During the transition, individual vesicles were released from the vesicle coacervate into the solution, which slightly increased the concentration of the *trans*-Azo units in the solution as well as the peak absorbance.

Eventually, we hoped to control the dimension of the vesicle aggregates through the adjustment of the vesicle

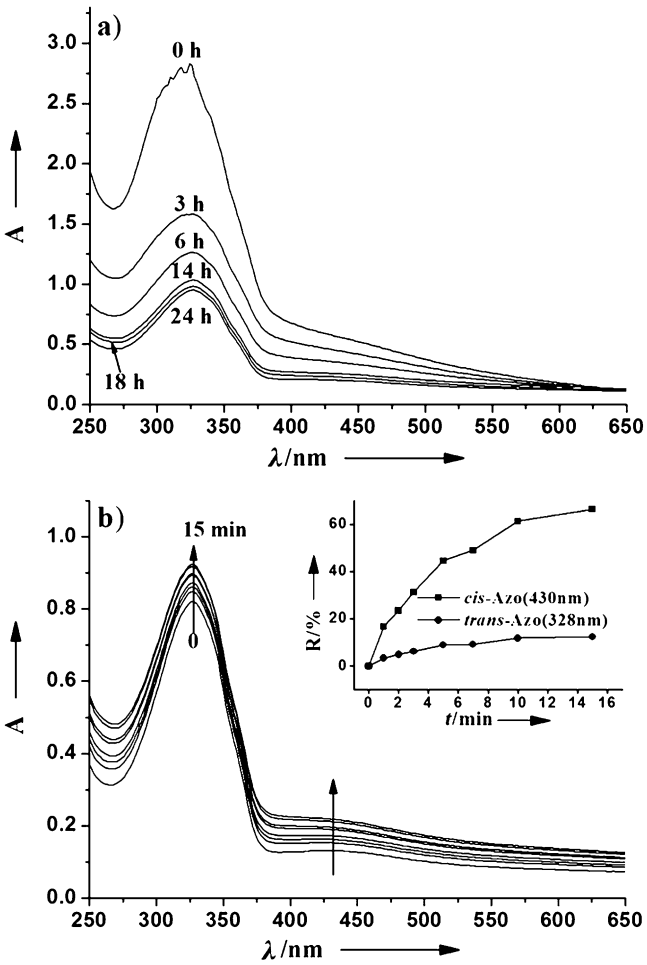

Figure 3. a) UV/Vis spectra of the vesicle mixture from CD-BPs and Azo-BPs under the irradiation of visible light at different time points. b) UV/Vis spectra of the vesicle coacervate mixture from CD-BPs and Azo-BPs under the irradiation of UV light at different time points.

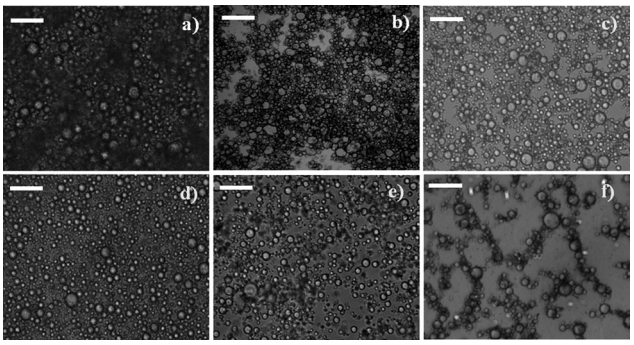

Figure 4. Vesicle aggregates at variable concentrations of polymers and CD groups: a) 5 mg mL^{-1}, 5×10^{-4} M; b) 2.5 mg mL^{-1}, 5×10^{-4} M; c) 1.25 mg mL^{-1}, 5×10^{-4} M; d) 5 mg mL^{-1}, 2.5×10^{-4} M; e) 2.5 mg mL^{-1}, 2.5×10^{-4} M; f) 1.25 mg mL^{-1}, 2.5×10^{-4} M. Scale bars: 25 μm.

concentration or composition. For such experiments, we changed the concentration of HBPO-star-PEO (namely the vesicle concentration) and that of either **1** or **2**, while keeping the molar ratio between the CD and Azo groups at 1:0.84. The results are shown in Figure 4. It can be concluded that with a decrease in the concentration of the vesicles (images from left to right in each row; Figure 4) and the recognition molecules (images from top to bottom in each column; Figure 4), the density of the vesicle aggregates decrease accordingly. For example, the vesicle aggregates changed from the 3D macroscopic materials (Figure 4a) to the 2D self-assembled vesicle monolayer (Figure 4c), and even to the 1D vesicle chains (Figure 4f) when the polymer concentration decreased from 5 mg mL^{-1} to 1.25 mg mL^{-1} and the CD concentration decreased from 5×10^{-4} M to 2.5×10^{-4} M.

In conclusion, as a mimic for cell aggregation, we have prepared large-scale vesicle aggregates by using hyperbranched polymer vesicles as the building blocks, and light-responsive multivalent host–guest molecular recognition between β-cyclodextrin and azobenzene units as the driving force. The vesicle aggregates are stable for at least half a year and can be reversibly disassembled or re-assembled under alternating UV and Vis irradiation cycles. Meanwhile, the membrane fusion induced by the host–guest recognition is accompanied by the vesicle aggregation process according to the real-time observation, content mixing assays, and component mixing assays. Both the dimensions and densities of the vesicle aggregates can be controlled by adjusting the vesicle concentration or composition. The work has demonstrated that hyperbranched polymer vesicles are advantageous in constructing multivalent intervesicular interactions to realize large-scale, highly efficient, reversible, and stable vesicle aggregation. We anticipate that the intelligent porous macroscopic materials presented herein may find applications in biomedical field such as tissue engineering materials.

Received: May 9, 2011
Published online: September 9, 2011

Keywords: aggregation · cytomimetic · host-guest system · UV/Vis spectroscopy · vesicles

[1] a) R. O. Hynes, A. D. Lander, *Cell* **1992**, *68*, 303–322; b) L. Petruzzelli, M. Takami, H. D. Humes, *Am. J. Med.* **1999**, *106*, 467–476; c) G. De Saint Basile, G. Ménasché, A. Fischer, *Nat. Rev. Immunol.* **2010**, *10*, 568–579.

[2] a) F. M. Menger, K. D. Gabrielson, *Angew. Chem.* **1995**, *107*, 2260–2278; *Angew. Chem. Int. Ed. Engl.Angew. Chem. Int. Ed.* **1995**, *34*, 2091–2106; b) F. M. Menger, M. I. Angelova, *Acc. Chem. Res.* **1998**, *31*, 789–797.

[3] a) V. Marchi-Artzner, T. Gulik-Krzywicki, M. A. Guedeau-Boudeville, C. Gosse, J. M. Sanderson, J. C. Dedieu, J.-M. Lehn, *ChemPhysChem* **2001**, *2*, 367–376; b) V. Marchi-Artzner, L. Jullien, T. Gulik-Krzywicki, J.-M. Lehn, *Chem. Commun.* **1997**, 117–118.

[4] a) F. M. Menger, V. A. Seredyuk, A. A. Yaroslavov, *Angew. Chem.* **2002**, *114*, 1406–1408; *Angew. Chem. Int. Ed.* **2002**, *41*, 1350–1352; b) F. M. Menger, V. A. Seredyuk, *J. Am. Chem. Soc.* **2003**, *125*, 11800–11801; c) F. M. Menger, H. L. Zhang, *J. Am. Chem. Soc.* **2006**, *128*, 1414–1415.

[5] a) Z. Sideratou, J. Foundis, D. Tsiourvas, I. P. Nezis, G. Papadimas, C. M. Paleos, *Langmuir* **2002**, *18*, 5036–5039; b) I. Tsogas, D. Tsiourvas, G. Nounesis, C. M. Paleos, *Langmuir* **2005**, *21*, 5997–6001; c) I. Tsogas, D. Tsiourvas, G. Nounesis, C. M. Paleos,

Langmuir **2006**, *22*, 11322 – 11328; d) C. M. Paleos, D. Tsiourvas, Z. Sideratou, *ChemBioChem* **2011**, *12*, 510 – 521.
[6] a) J. Voskuhl, B. J. Ravoo, *Chem. Soc. Rev.* **2009**, *38*, 495 – 505; b) B. J. Ravoo, J. C. Jacquier, G. Wenz, *Angew. Chem.* **2003**, *115*, 2112 – 2116; *Angew. Chem. Int. Ed.* **2003**, *42*, 2066 – 2070; c) C. W. Lim, B. J. Ravoo, D. N. Reinhoudt, *Chem. Commun.* **2005**, 5627 – 5629; d) S. K. M. Nalluri, B. J. Ravoo, *Angew. Chem.* **2010**, *122*, 5499 – 5502; *Angew. Chem. Int. Ed.* **2010**, *49*, 5371 – 5374.
[7] a) R. J. Mart, K. P. Liem, X. Wang, S. J. Webb, *J. Am. Chem. Soc.* **2006**, *128*, 14462 – 14463; b) P. L. Kwan, R. J. Mart, S. J. Webb, *J. Am. Chem. Soc.* **2007**, *129*, 12080 – 12081; c) R. J. Mart, K. P. Liem, S. J. Webb, *Pharm. Res.* **2009**, *26*, 1701 – 1710.
[8] H.-K. Lee, K. M. Park, Y. J. Jeon, D. Kim, D. H. Oh, H. S. Kim, C. K. Park, K. Kim, *J. Am. Chem. Soc.* **2005**, *127*, 5006 – 5007.
[9] a) L. Zhang, A. Eisenberg, *Science* **1995**, *268*, 1728 – 1731; b) L. Zhang, K. Yu, A. Eisenberg, *Science* **1996**, *272*, 1777 – 1779; c) B. M. Discher, Y. Y. Won, D. S. Ege, J. Lee, F. S. Bates, D. E. Discher, D. A. Hammer, *Science* **1999**, *284*, 1143 – 1146; d) D. E. Discher, A. Eisenberg, *Science* **2002**, *297*, 967 – 973; e) M. Antonietti, S. Förster, *Adv. Mater.* **2003**, *15*, 1323 – 1333; f) D. A. Hammer, G. P. Robbins, J. B. Haun, J. J. Lin, W. Qi, L. A. Smith, P. P. Ghoroghchian, M. J. Therien, F. S. Bates, *Faraday Discuss.* **2008**, *139*, 129 – 141.
[10] P. J. Photos, L. Bacakova, B. Discher, F. S. Bates, D. E. Discher, *J. Controlled Release* **2003**, *90*, 323 – 334.
[11] a) J. J. Lin, P. Ghoroghchian, Y. Zhang, D. A. Hammer, *Langmuir* **2006**, *22*, 3975 – 3979; b) G. P. Robbins, R. L. Saunders, J. B. Haun, J. Rawson, M. J. Therien, D. A. Hammer, *Langmuir* **2010**, *26*, 14089 – 14096; c) G. P. Robbins, D. Lee, J. S. Katz, P. R. Frail, M. J. Therien, J. C. Crocker, D. A. Hammer, *Soft Matter* **2011**, *7*, 769 – 779.
[12] a) A. Bhattacharya, A. C. Balazs, *J. Mater. Chem.* **2010**, *20*, 10384 – 10396; b) G. V. Kolmakov, V. V. Yashin, S. P. Levitan, A. C. Balazs, *Proc. Natl. Acad. Sci. USA* **2010**, *107*, 12417 – 12422.
[13] T. P. Smart, C. Fernyhough, A. J. Ryan, G. Battaglia, *Macromol. Rapid Commun.* **2008**, *29*, 1855 – 1860.
[14] a) Y. F. Zhou, D. Y. Yan, *Angew. Chem.* **2004**, *116*, 5004 – 5007; *Angew. Chem. Int. Ed.* **2004**, *43*, 4896 – 4899; b) Y. F. Zhou, D. Y. Yan, W. Y. Dong, Y. Tian, *J. Phys. Chem. B* **2007**, *111*, 1262 – 1270.
[15] a) Y. F. Zhou, D. Y. Yan, *J. Am. Chem. Soc.* **2005**, *127*, 10468 – 10469; b) Y. F. Zhou, D. Y. Yan, *Angew. Chem.* **2005**, *117*, 3287 – 3290; *Angew. Chem. Int. Ed.* **2005**, *44*, 3223 – 3226.
[16] a) Y. F. Zhou, W. Huang, J. Y. Liu, X. Y. Zhu, D. Y. Yan, *Adv. Mater.* **2010**, *22*, 4567 – 4590; b) C. M. Paleos, D. Tsiourvas, Z. Sideratou, *Gene Ther. Mol. Biol.* **2007**, *11*, 117 – 132.
[17] a) A. Ueno, H. Yoshimura, R. Saka, T. Osa, *J. Am. Chem. Soc.* **1979**, *101*, 2779 – 2780; b) A. Harada, *Acc. Chem. Res.* **2001**, *34*, 456 – 464; c) S. Yagai, A. Kitamura, *Chem. Soc. Rev.* **2008**, *37*, 1520 – 1529; d) X. Liao, G. Chen, X. Liu, W. Chen, F. Chen, M. Jiang, *Angew. Chem.* **2010**, *122*, 4511 – 4515; *Angew. Chem. Int. Ed.* **2010**, *49*, 4409 – 4413; e) X. Liu, M. Jiang, *Angew. Chem.* **2006**, *118*, 3930 – 3934; *Angew. Chem. Int. Ed.* **2006**, *45*, 3846 – 3850; f) Y. Wang, N. Ma, Z. Wang, X. Zhang, *Angew. Chem.* **2007**, *119*, 2881 – 2884; *Angew. Chem. Int. Ed.* **2007**, *46*, 2823 – 2826.
[18] F. M. Winnik, *Chem. Rev.* **1993**, *93*, 587 – 614.
[19] a) J. Wilschut, N. Duzgunes, R. Fraley, D. Papahadjopoulos, *Biochemistry* **1980**, *19*, 6011 – 6021; b) H. R. Marsden, I. Tomatsu, A. Kros, *Chem. Soc. Rev.* **2011**, *40*, 1572 – 1585.
[20] P. Somerharju, *Chem. Phys. Lipids* **2002**, *116*, 57 – 74.

